ACADEMIC
PRESS

Experimental investigations of the response of a cracked rotor to periodic axial excitation

A.K. Darpe, K. Gupta*, A. Chawla

Department of Mechanical Engineering, Indian Institute of Technology, Hauz Khas, Delhi 110016, India

Abstract

In this paper, the coupling of lateral and longitudinal vibrations due to the presence of transverse surface crack in a rotor is explored. A crack in a rotor is known to introduce coupling between lateral and longitudinal vibrations. Steady state unbalance response of a cracked rotor with a single centrally situated crack subjected to periodic axial impulses is investigated experimentally. The cracked rotor is excited axially using an electrodynamic exciter at a frequency equal to its bending natural frequency in both non-rotating and rotating conditions. The resulting time domain and frequency domain signals of the cracked rotor are studied. Spectral response of the cracked rotor with and without axial excitation is found to be distinctively different. When excited axially, it shows prominent presence of rotor bending natural frequency. However for an uncracked rotor, the response is similar with or without axial excitation. It is thus proposed that the response of the rotor to axial impulse excitation could be used for more reliable diagnosis of rotor cracks.
© 2002 Elsevier Science Ltd. All rights reserved.

1. Introduction

Fatigue cracks are a potential source of catastrophic failures in rotors. Researchers have put in considerable effort to develop a foolproof and reliable strategy to detect cracks in rotors. One of the approaches investigated in detail is the phase and amplitude variation in the $2x$ component of steady state (unbalance) response. Several authors [1–7] have focused their attention on $1x$ and $2x$ components of rotor vibration and discussed the effect of crack on these frequency components. However, it is known that even for shallow to moderate cracks, the presence of $2x$ component of vibration cannot be considered as a reliable indicator of the presence of a crack in the rotor. This is because there are several other mechanisms that generate the second harmonic ($2x$) component.

---

*Corresponding author. Tel.: +91-116-591122; fax: +91-116-851169.

E-mail address: kgupta@mech.iitd.ernet.in (K. Gupta).

A recent approach to this problem has been to study the coupling between lateral, axial and torsional vibrations caused by the presence of a crack in a rotor. Papadopoulos and Dimarogonas [8] studied coupling of bending and torsional vibrations of cracked Timoshenko shaft with an open-crack assumption. Presence of bending vibration frequencies in torsional spectra had been cited as potential crack indicators. Muszynska et al. [9] analysed torsional/lateral cross-coupled vibration response. Ostachowicz and Krawczuk [10] analysed coupled torsional and bending vibrations of a rotor with an open crack using finite element model. They analysed the effect of external torsional moment on lateral vibrations of cracked rotor due to coupling effect of crack. Papadopoulos and Dimarogonas [11] studied coupling of lateral and longitudinal vibrations and have proposed co-existence of lateral and longitudinal vibration frequencies in the same spectrum as an unambiguous crack indicator. They have shown that there exists instability between forward and backward critical speeds as well as at the critical speed corresponding to the longitudinal eigenvalue of the shaft.

Papadopoulos and Dimarogonas [12] have observed a strong coupling of longitudinal and lateral vibrations and of lateral and torsional vibrations even for relatively small crack depths of 6% using sweep excitation. They have used a clamped–free Timoshenko shaft with an open-crack model. Papadopoulos and Dimarogonas [13] have studied the stability of cracked shafts in coupled vibration mode. Effect of closing crack was taken into account by representing variation in stiffness in the form of a truncated cosine series. They have reported a case study on 300 MW steam turbine, wherein the lateral vibration spectrum showed subharmonics of fundamental longitudinal natural frequency. They also experimentally verified this coupling phenomenon on a clamped–free (non-rotating) shaft by using sweep harmonic excitation [14]. The longitudinal natural frequencies appeared in the lateral vibration spectrum and the lateral natural frequencies appeared in the longitudinal frequency spectrum as the excitation frequency is swept over a wide frequency range. To the authors' best knowledge, this is the only experimental work on coupled vibrations of cracked shaft.

Iwatsubo et al. [15] used external excitation technique experimentally and applied it to the cracked shaft but did not consider coupling of vibrations. They used lateral periodic and impact excitation and analysed the lateral response of the cracked rotor. They suggested the presence of combination harmonics due to interaction between impact force and rotation of shaft as crack indicators. In an analytical work, Collins et al. [16] studied detection of cracks using axial impulses to a rotating Timoshenko shaft. They also reported the presence of combination harmonics in the lateral vibration spectrum. The rotor speed considered was above half the critical speed and the amplitude of the running frequency was found to be dominant in comparison to the sum and difference frequency components. Darpe et al. [17] have studied the coupling of bending and axial vibrations in a slow rotating cracked Jeffcott rotor using periodic axial impulse excitation. Predominant existence of lateral bending natural frequency, axial excitation frequency and side bands around it in lateral vibration spectrum have been shown as important crack indicators. From the literature, no work could be found on the experimental investigations of rotating cracked shafts utilising the phenomenon of coupling between bending-axial vibrations. If such a coupling of vibrations can be identified on a rotating cracked shaft and duly correlated with the crack on the shaft, it could be of considerable practical significance.

In this paper, response of a cracked rotor with a centrally situated transverse surface crack subjected to external axial excitation is investigated experimentally. External excitation is in the

form of periodic axial impulses. If the axial vibration frequencies coexist with lateral vibration frequencies in the lateral vibration spectrum, it would confirm the existence of coupling of axial–bending vibrations in the rotor, which in absence of any other coupling mechanisms, will be a reliable indicator of presence of crack. Comparison with the response of the uncracked shaft to similar excitation is made. Darpe et al. [17] have carried out detailed analytical investigations on the axial–bending coupling in a rotating cracked shaft and have shown the existence of important crack indicators based on this coupling phenomenon. The objective of the present experimental work is to verify the theoretical findings reported in Ref. [17] and to understand the phenomenon of coupling of bending–axial vibration for possible application to detection of cracks in rotors. However, equations of motion and some of the important results reported in Ref. [17] are discussed here in the following section for the sake of completeness in theoretical background before presenting the experimental results.

The application of compressive axial impulses to the rotor causes high-frequency axial vibrations. The overall state of stress on the crack edge due to the transverse and axial forces decides the status of crack (open or close). Coupled equations of motion involving longitudinal displacement and two (vertical and horizontal) lateral displacements are considered. The response to single and multiple impulses per rotation are computed by numerically integrating the equations of motion using Runge–Kutta method. Frequency spectra of vertical and horizontal lateral rotor vibrations are studied in detail.

2. Response of a Jeffcott rotor to axial impulses

Consider a massless elastic shaft of diameter D and length L with a disc of mass m mounted at mid-span. The co-ordinates y, z and ξ, η represent the stationary and rotating axes, respectively, as shown in Fig. 1. The co-ordinate u represents longitudinal axis. The eccentricity of the centre of the disc mass m from the geometric centre of the disc is ε and β is the orientation of the eccentricity in the direction of the shaft rotation from ξ axis. $\theta(t)$ is the instantaneous angle of rotation and ω is the rotational speed. The damping coefficient is c.

Jun et al. [6] discussed the breathing crack model and that model is extended here by including the axial co-ordinate. Considering direct stiffnesses k_ξ, k_η and k_u in the ξ, η and u directions, and cross-coupled stiffnesses $k_{\xi\eta}$, $k_{\eta\xi}$, $k_{\xi u}$, $k_{\eta u}$, $k_{u\xi}$ and $k_{u\eta}$ which come into play due to partial opening of the crack, the equations of motion can be expressed in the rotating co-ordinates as [18]

$$m(\ddot{\xi} - 2\omega\dot{\eta} - \omega^2\xi) + c(\dot{\xi} - \omega\eta) + k_\xi\xi + k_{\xi\eta}\eta + k_{\xi u}u = m\varepsilon\omega^2\cos\beta - mg\cos\theta,$$
$$m(\ddot{\eta} + 2\omega\dot{\xi} - \omega^2\eta) + c(\dot{\eta} + \omega\xi) + k_{\eta\xi}\xi + k_\eta\eta + k_{\eta u}u = m\varepsilon\omega^2\sin\beta + mg\sin\theta,$$
$$m\ddot{u} + c\dot{u} + k_{u\xi}\xi + k_{u\eta}\eta + k_u u = 0. \tag{1}$$

As evident from the above equations, the longitudinal displacement u is coupled to the lateral displacements ξ and η through the cross-coupled stiffness terms $k_{u\xi}$ and $k_{u\eta}$. Stiffnesses in the equations of motion (1) are response dependent, resulting in non-linear differential equations. The response itself depends upon the stiffness values used in the equation of motion. The response influences the forces acting on the cracked cross-section and that in turn influences the state of
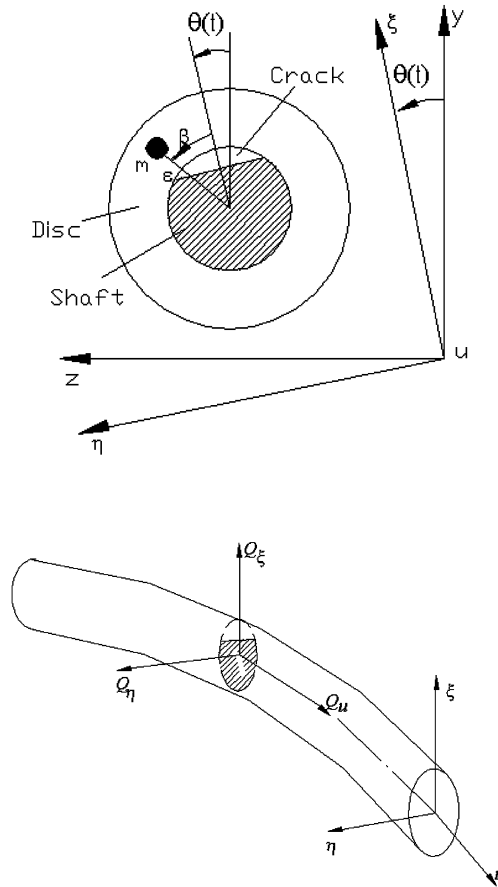
Fig. 1. The co-ordinate system and the forces acting on the crack cross-section.

stress on the crack edge. The stress field on the crack edge is indicated by the stress intensity factor (SIF) which is a function of forces acting on the crack edge. Negative SIF indicates compressive stress field and the crack is closed at that point along the crack tip, whereas positive SIF indicates tensile stress field and the crack in open state. The stiffness depends on the amount of crack opening and the same can be estimated from the stress field along the crack tip. This is how the response and stiffness are interdependent leading to the non-linear equations that are therefore solved numerically.

Equations of motion (1) can be non-dimensionalised using the following non-dimensional parameters:

$$\bar{\xi} = \xi/\delta_{st}, \quad \bar{\eta} = \eta/\partial_{st}, \quad \bar{u} = u/\delta_{st}, \quad \zeta = \frac{c}{2\sqrt{k_0 m}}, \quad \tau = \omega t, \quad e = \varepsilon/\delta_{st}, \quad \bar{a} = a/D,$$

$$r_0 = \omega_0/\omega, \quad r_\xi = \omega_\xi/\omega, \quad r_\eta = \omega_\eta/\omega, \quad r_u = \omega_u/\omega, \quad r_{unb} = \omega/\omega_0,$$

$$r_{\xi u} = \omega_{\xi u}/\omega, \quad r_{u\xi} = \omega_{u\xi}/\omega, \quad r_{\eta u} = \omega_{\eta u}/\omega, \quad r_{u\eta} = \omega_{u\eta}/\omega, \quad r_{\xi\eta} = \omega_{\xi\eta}/\omega, \quad r_{\eta\xi} = \omega_{\eta\xi}/\omega,$$

where

$$\delta_{st} = mg/k_0, \quad \omega_0 = \sqrt{\frac{k_0}{m}}, \quad \omega_\xi = \sqrt{\frac{k_\xi}{m}}, \quad \omega_\eta = \sqrt{\frac{k_\eta}{m}}, \quad \omega_u = \sqrt{\frac{k_u}{m}},$$

$$\omega_{\xi u} = \sqrt{\frac{k_{\xi u}}{m}}, \quad \omega_{u\xi} = \sqrt{\frac{k_{u\xi}}{m}}, \quad \omega_{\eta u} = \sqrt{\frac{k_{\eta u}}{m}}, \quad \omega_{u\eta} = \sqrt{\frac{k_{u\eta}}{m}}, \quad \omega_{\xi \eta} = \sqrt{\frac{k_{\xi \eta}}{m}}, \quad \omega_{\eta \xi} = \sqrt{\frac{k_{\eta \xi}}{m}}. \quad (2)$$

Here k_0 is the stiffness of the shaft without crack. Equations of motion in non-dimensional form are

$$\ddot{\bar{\xi}} + 2\zeta r_0 \dot{\bar{\xi}} - 2\dot{\bar{\eta}} + (r_\xi^2 - 1)\bar{\xi} + (r_{\xi\eta}^2 - 2\zeta r_0)\bar{\eta} + r_{\xi u}^2 \bar{u} = e\cos\beta - r_0^2 \cos\tau,$$

$$\ddot{\bar{\eta}} + 2\zeta r_0 \dot{\bar{\eta}} + 2\dot{\bar{\xi}} + (r_\eta^2 - 1)\bar{\eta} + (r_{\eta\xi}^2 + 2\zeta r_0)\bar{\xi} + r_{\eta u}^2 \bar{u} = e\sin\beta + r_0^2 \sin\tau,$$

$$\ddot{\bar{u}} + 2\zeta r_0 \dot{\bar{u}} + r_{u\xi}^2 \bar{\xi} + r_{u\eta}^2 \bar{\eta} + r_u^2 \bar{u} = 0. \quad (3)$$

The solution process for solving the above equations of motion is iterative, quite involved and has been detailed in Ref. [17]. However it is set forth below in brief.

Eq. (3) is integrated using fourth order Runge–Kutta procedure. A program in MATLAB (version 5.3) is written to implement the solution procedure. Stiffnesses are assumed to be constant for one degree of rotation ($\pi/180$ rad), for which the integration of Eq. (3) is carried out with sufficiently small time step ($\Delta t = 0.00001445$ s) for accurate solution. The response obtained at the end of one degree of rotation is stored and used to calculate forces acting on the crack cross-section (Fig. 1) using the following equation:

$$Q_\xi = k_\xi \xi + k_{\xi\eta}\eta + k_{\xi u}u,$$

$$Q_\eta = k_{\eta\xi}\xi + k_\eta\eta + k_{\eta u}u,$$

$$Q_u = k_{u\xi}\xi + k_{u\eta}\eta + k_u u. \quad (4)$$

These forces are used to find the SIF [17] at 50 different points along the crack edge and the sign of these at these points decides the extent of open part of the crack. The open part of the crack contributes to the additional flexibility of the cracked rotor and influence the new values of stiffness k_ξ, k_η, k_u, $k_{\xi\eta}$, $k_{\eta\xi}$, $k_{\xi u}$, $k_{\eta u}$, $k_{u\xi}$ and $k_{u\eta}$. These new stiffness values are used in Eq. (3) to estimate the next set of displacements ($\bar{\xi}, \bar{\eta}$ and $\bar{u}$). Thus the response is used to evaluate stiffnesses, which in turn give next set of response. To attain a steady state, the iterative procedure is repeated till the response set for one full rotation is converged. The tolerance for convergence of response is taken to be of the order of 0.1%. After initial transients in the response die within first few rotor rotations, steady state stabilised solution is obtained (refer to Ref. [17] for the detailed solution process).

To apply the axial impulse in theoretical simulation, the axial velocity at that instant is decreased by $\Delta\dot{u} = 800$. For single axial impulse per rotation, the axial velocity is decreased when the rotor is in reference position, i.e., $\theta = 0°$, whereas for multiple impulses, $\Delta\dot{u}$ is implemented after every $360/i$ degree of rotation, i being the number of impulses per rotation.

Initially, a cracked rotor with crack depth ratio $\bar{a} = 0.2$ is analysed for $r_{unb} = 0.1$ without subjecting it to axial impulse excitation. The corresponding frequency spectrum (Fig. 2) shows rotational frequency ($1x$) and its harmonics ($2x$, $3x$) with decreasing amplitude. The response of an uncracked rotor under similar conditions (not shown here) shows only rotational frequency
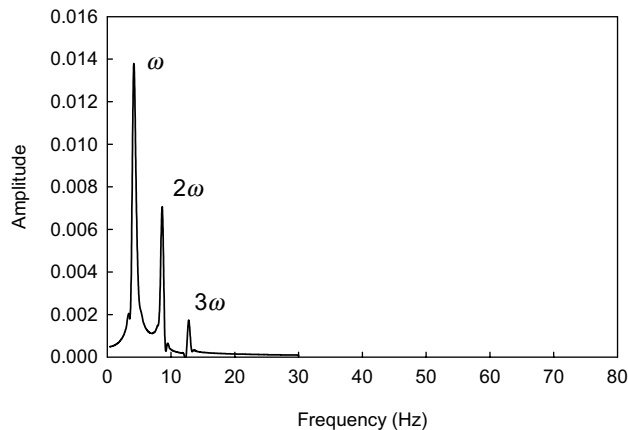
Fig. 2. Frequency spectrum of rotor vibration (vertical) of cracked rotor without external axial impulses ($\bar{a} = 0.2$, $r_{unb} = 0.1$).

components with the absence of higher harmonic components which is obvious. Next the effect of axial excitation on both uncracked and cracked rotors is studied. To analyse the transient response to application of an impulse, the uncracked rotor is subjected to only a single impulse applied at $\tau = 6.28$ (at the end of the first rotation). The effect of axial impulse is not seen in the lateral response of the uncracked rotor (Fig. 3a). The response after the application of impulse ($\tau > 6.28$) is the same as the response before the application of impulse ($\tau < 6.28$). However, when a cracked rotor ($\bar{a} = 0.2$) is subjected to similar single impulse (applied at $\tau = 6.28$), the transient bending vibration response (Fig. 3c) is clearly quite different compared to the uncracked rotor case. The response to this solitary impulse obviously dies after few rotations since the impulse is not repeated again. However, the high-frequency vibrations are obvious in the transient response just after the application of impulse. A close view of the time domain response shown in Fig. 3c reveals a 10ω frequency component (which matches with the bending natural frequency ω_0 of the rotor). In order to assess the effect of application of single impulse (not single impulse per rotation) on the rotor's response, the FFT of the transient response (from $\tau = 6.28$ to 44.26) is obtained (Fig. 3d). This spectrum shows the prominent presence of bending natural frequency along with rotational frequency. This bending natural frequency is absent in the spectrum of uncracked rotor response (Fig. 3b).

When the same rotor is subjected to a single impulse per rotation (periodic impulse excitation), several harmonics are seen in the frequency spectrum (Fig. 4a), the prominent being the rotor bending natural frequency (42.7 Hz). This is because when single impulse per rotation is applied, the excitation frequencies in axial direction include axial excitation frequency (equal to rotational frequency) and its higher harmonics. One of the higher harmonics, because of coupling between axial and bending vibrations in a cracked rotor, excites resonant bending vibrations leading to the presence of bending natural frequency in the spectrum.

Next instead of a single impulse, several impulses are applied per rotation. Rotational speed is kept the same, at $r_{unb} = 0.1$. Fig. 4b shows the frequency spectrum of cracked rotor ($\bar{a} = 0.2$) vibration when the rotor is subjected to 4 impulses per rotation, the impulse excitation frequency
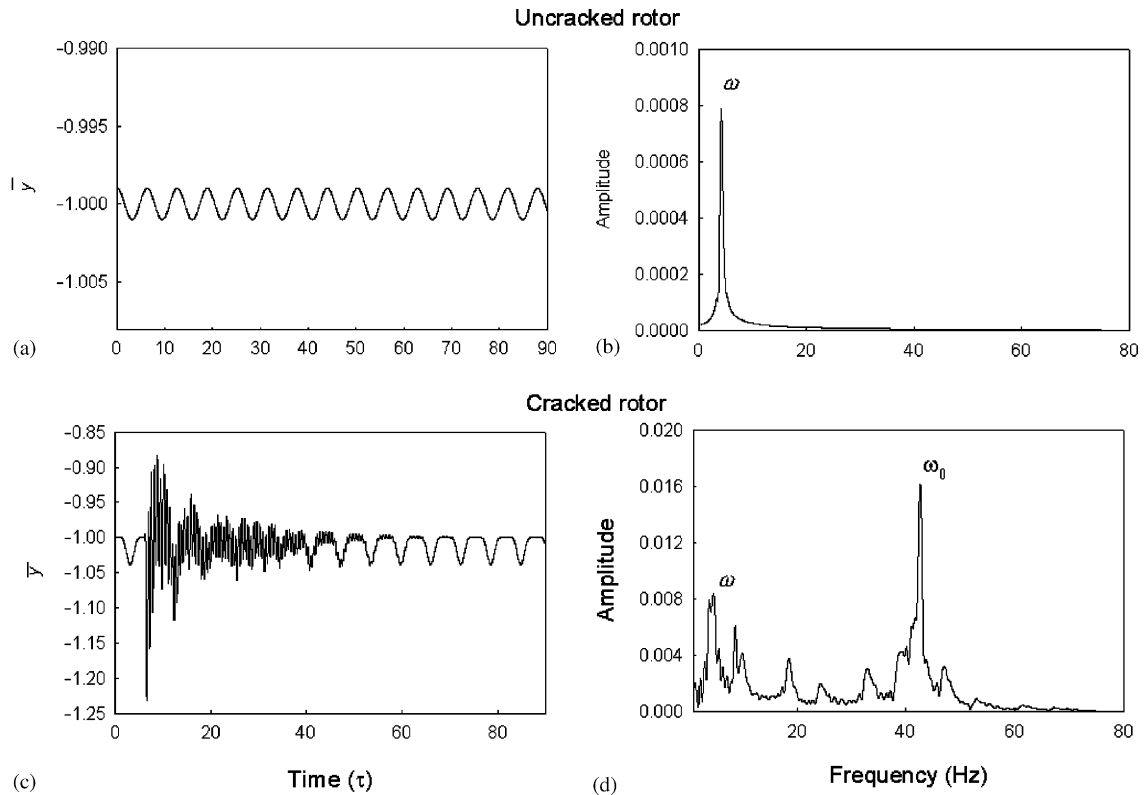
Fig. 3. Rotor response to a single impluse applied at $\tau = 6.28$. $r_{unb} = 0.1$. (a) and (b) uncracked rotor; (c) and (d) cracked rotor with $\bar{a} = 2$. (a,c) time domain and (b,d) frequency domain response.
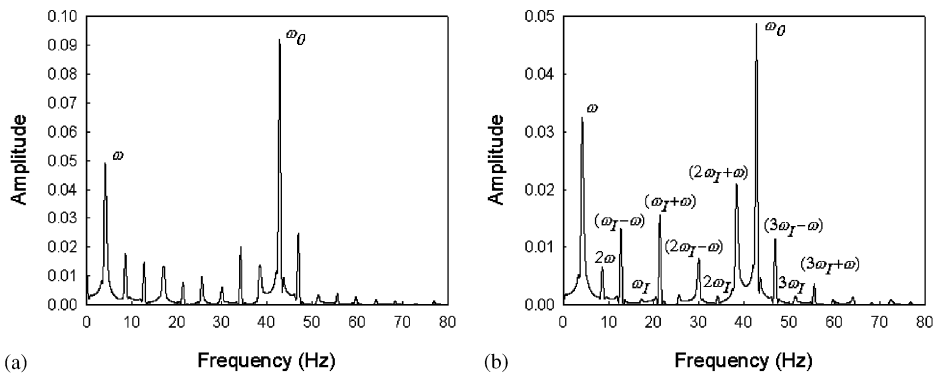

Fig. 4. Frequency spectrum of rotor vibration due to (a) single impulse per rotation ($\omega_I = 4.27$ Hz): and (b) 4 impulses per rotation ($w_I = 17$ Hz). $\bar{a} = 0.2$, $r_{unb} = 0.1$.

ω_I being 4ω. The excitation frequencies in the spectrum of this case are the rotor running frequency ω (unbalance excitation) and the impulse excitation frequency ω_I, as well as its harmonics ($2\omega_I$, $3\omega_I$, etc.). The axial excitation with $4x$ frequency (ω_I) and its harmonics ($2\omega_I$,
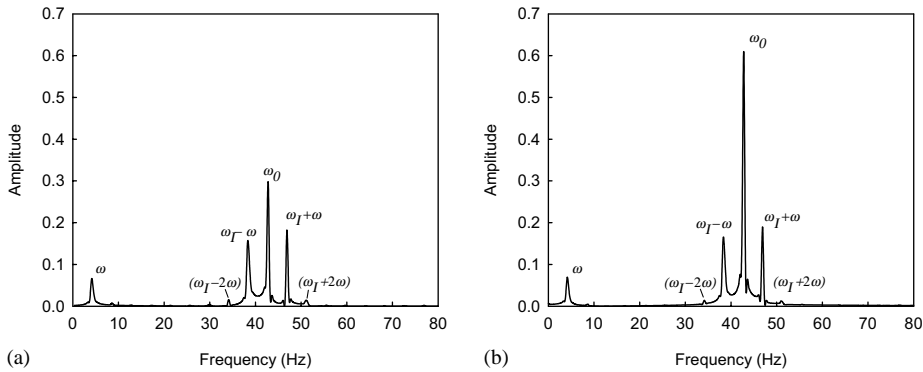
Fig. 5. Frequency spectrum of rotor vibration due to 10 impulses per rotation ($\omega_I = 42.7\,\text{Hz}$): (a) vertical; (b) horizontal. $\bar{a} = 0.2$, $r_{unb} = 0.1$.

$3\omega_I$, etc.) interact with unbalance excitation frequency (ω) to produce sum and difference frequencies $n\omega_I + \omega$ and $n\omega_I - \omega$. The rotor vibration with high-frequency $n\omega_I$ is modulated by a low unbalance excitation frequency ω. The spectrum hence shows the combination harmonics such as $\omega_I + \omega$, $\omega_I - \omega$, $2\omega_i + \omega$, $2\omega_I - \omega$ and so on. The bending natural frequency ω_0 is also prominently seen in the spectrum although neither ω_I nor any of its higher harmonics matches ω_0. This is because another lateral vibration frequency component 2ω, which exists owing to non-linearity due to crack, also modulates $n\omega_I$, thus giving rise to the presence of $n\omega_I \pm 2\omega$ components in the spectra. The component $2\omega_I + 2\omega$ being equal to ω_0, resonance condition is effected and hence the presence of bending natural frequency in the spectrum.

The number of impulses are now increased to 10 impulses per rotation so as to match impulse excitation frequency (ω_I) with the bending natural frequency (ω_0). The bending natural frequency (ω_0) component in the frequency spectra is much more prominent along with the sum and difference frequency components (Fig. 5a and b). The figures also show stronger natural frequency component in the horizontal direction compared to the vertical direction.

3. Experimental setup

To understand the phenomenon of coupling between bending and axial vibrations of a cracked rotor, a test rig that comprises a cracked rotor with a central disc, a driving unit, an electrodynamic exciter and measurement, signal processing, and data acquisition units (shown in Fig. 6) is developed.

A fatigue crack is induced on the shaft transversely using a three-point-fatigue bending machine. For this purpose a 25 mm diameter shaft is used with a very fine initial slit of width 0.5 mm and depth 1 mm using a jeweler's saw. This is to initiate a fatigue crack at a desired location. The shaft is then placed in a fatigue bending machine and subjected to a cyclic load. The crack growth is tracked on the polished outer surface using a magnifying lens. Once the crack propagates to a desired depth, the specimen is machined to a diameter of 15 mm. The machining
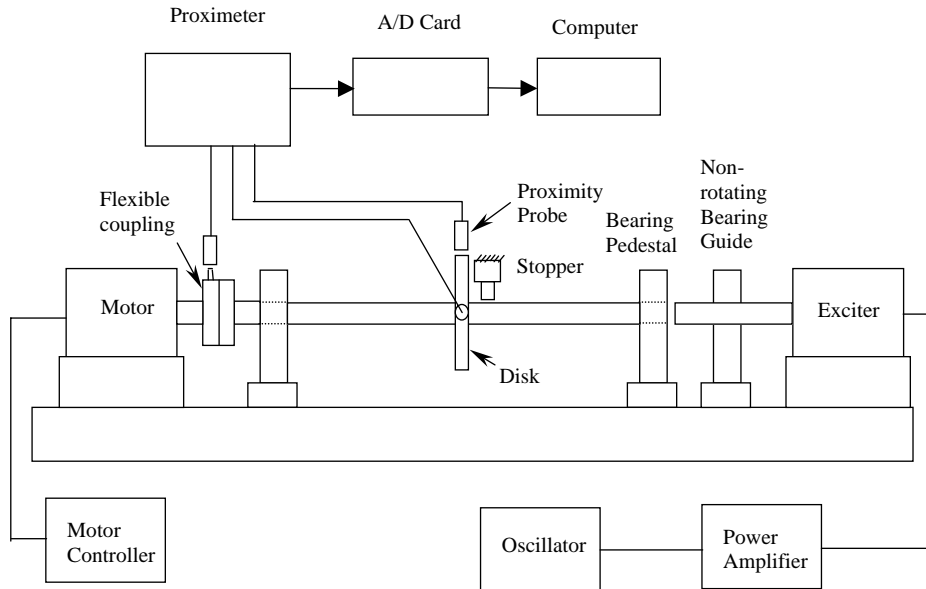
Fig. 6. Test rig with instrumentation.

thus removes the initial slit and a slight bow that may creep in during loading on the fatigue bending machine.

The shaft in the test rig is supported with a bearing span of 640 mm. A disc of mass 1 kg is mounted at mid-span and the rotor is then supported on self-aligning ball bearings (SKF #2201). The crack is located at a distance of 4 mm from the disc face. A flexible Lovejoy-type coupling connects the rotor with the drive motor. The drive motor is Siemens make 750 W 3 phase induction motor controlled by a Micromaster vector.

For vibration signal acquisition, the signal from the shaft in stationary non-rotating condition is acquired in either axial, vertical or horizontal direction from the central disc using an accelerometer (B&K make 4371). The signal from the accelerometer is sent to the A/D card through a charge amplifier. In rotating condition, however, the signal is acquired using non-contact-type eddy current probes. The signals from the probes are conditioned at the proximeter before sending them to the A/D card plugged on to a digital computer. A small Labview™ virtual instrument that facilitates in acquiring and storing the digitised data on the computer is developed. For the rotating case, the signals are acquired simultaneously from three proximity probes, two probes at the disc location (one each for horizontal and vertical shaft vibrations) and one near the coupling for keyphasor signal.

For exciting the shaft axially, an electrodynamic exciter is positioned horizontally and properly aligned with the shaft axis. To ensure that the excitation is purely axial, a push rod that extends the exciter plunger to the shaft end is guided in a carefully aligned non-rotating bearing pedestal positioned between the right end bearing housing of the shaft and the exciter. The exciter is fed an oscillating signal from the oscillator that can generate an electrical signal of a desired frequency either in sinusoidal or square waveform. A square pulse signal with pulse width equal to half the

cycle width and amplitude of 2.5 V is used to simulate an impulse excitation. The signal from the oscillator is amplified using a power amplifier.

4. Experimental results and discussion

Experiments with axial excitation are carried out in two steps. First the uncracked and the cracked shafts are excited in stationary (non-rotating) condition. This is to establish experimentally the coupling between the axial and bending vibrations in a cracked rotor and to check if it is really absent in the case of an uncracked rotor. The time domain response in axial direction measured on disc face also helps in ensuring that the intensity of axial impulses is equal or comparable in magnitude in both the cases of the uncracked and the cracked rotors. Next the axial excitation is repeated on the uncracked and cracked shafts in rotating condition. Unless otherwise stated, the axial excitation frequency is equal to the bending natural frequency of the rotor. In the case of the non-rotating shaft the vibration signal is picked up from an accelerometer mounted on the disc face for axial vibration. For transverse vibrations, i.e., in horizontal and vertical directions, the accelerometer is mounted on the disc periphery.

4.1. Non-rotating shaft

The bending natural frequency for the uncracked shaft is found to be 46.4 Hz. Fig. 7 shows the time domain and frequency domain signals of the uncracked shaft subjected to axial excitation at a frequency equal to the bending natural frequency of the shaft. The time domain signal in axial direction (Fig. 7a) shows sudden rise in the amplitude after a regular interval of time (approximately 21.5 ms) indicating the application of impulse at a frequency of 46.4 Hz. The frequency domain signal (Fig. 7b) shows the excitation frequency and its second harmonic in the spectrum. Time domain signal in horizontal direction shows the presence of high-frequency vibrations (Fig. 7c). It also shows a sudden rise in amplitude at regular interval that is due to the effect of axial excitation. The bending natural frequency (Fig. 7d) is observed in the frequency spectrum. The application of impulse is always followed by high-frequency vibrations that is evident in the time domain signal (Fig. 7a, c and e). From these time domain signals it should also be noted that the amplitude of vibration is much larger in axial direction (0.035 m/s pp approximately) than in vertical and horizontal directions (0.007 m/s pp approximately). This is due to the fact that the impulses are applied in the axial direction. The response in both the lateral directions is almost same in amplitude and frequency content. It may be noted that since there is no excitation in the transverse direction, the uncracked shaft ideally should not have shown the presence of bending natural frequency in the spectrum of horizontal or vertical vibration. However, its presence may be attributed to the impulse applied being not purely axial and/or the presence of some amount of residual bow in the shaft despite the best care taken to avoid the same.

Now similar impulses are applied to the cracked shaft of crack depth ratio of $\bar{a} = 0.23$. Here the axial vibration response (Fig. 8a) looks quite similar to that of the uncracked shaft. The spectrum contains excitation frequency and its harmonics (Fig. 8b). The application of impulses axially is clearly seen in the time domain signal in the form of periodic rise in amplitudes. However, the time
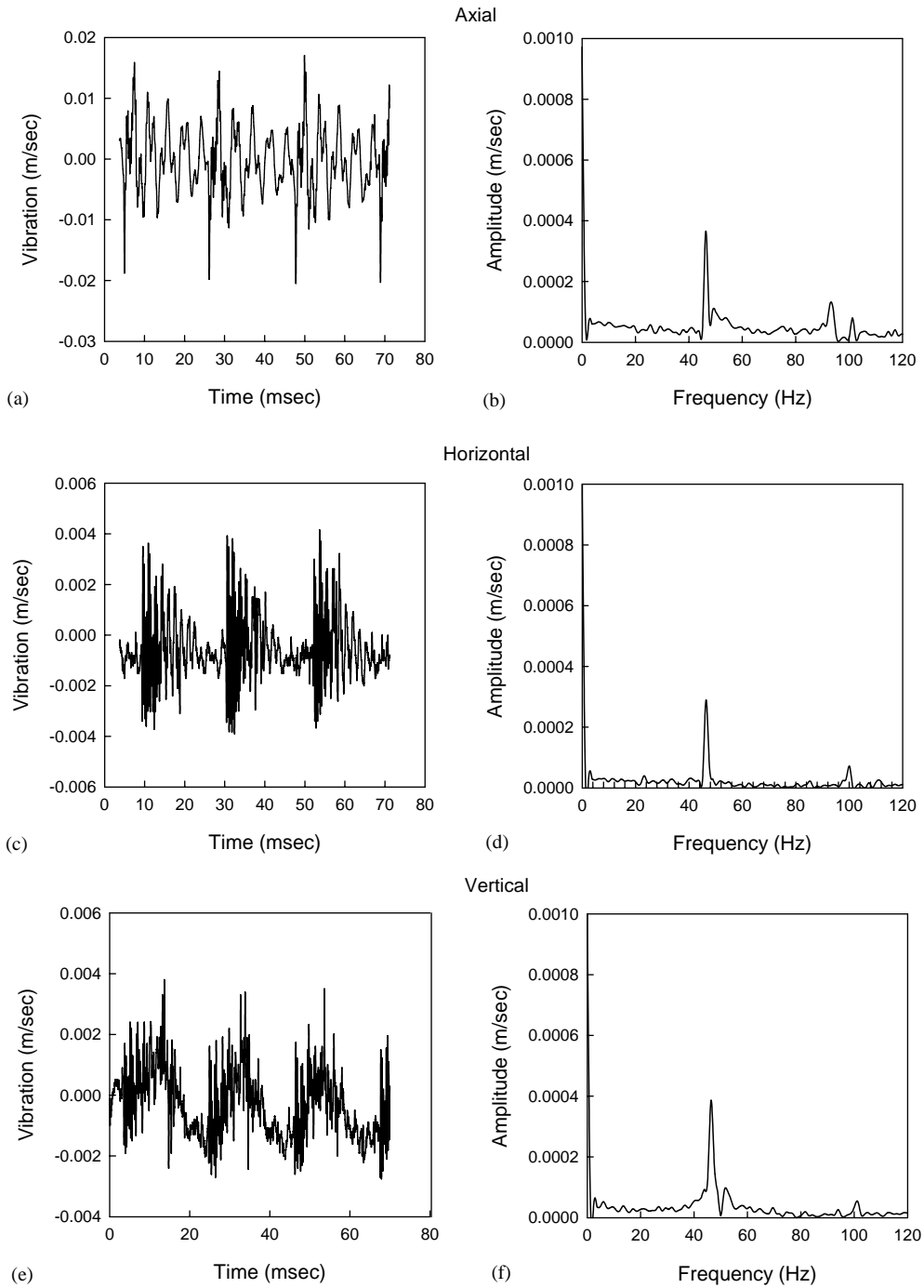
Fig. 7. Time domain and frequency domain response of solid shaft in non-rotating condition subjected to periodic impulse excitation: (a,b) axial; (c,d) horizontal; (e,f) vertical.
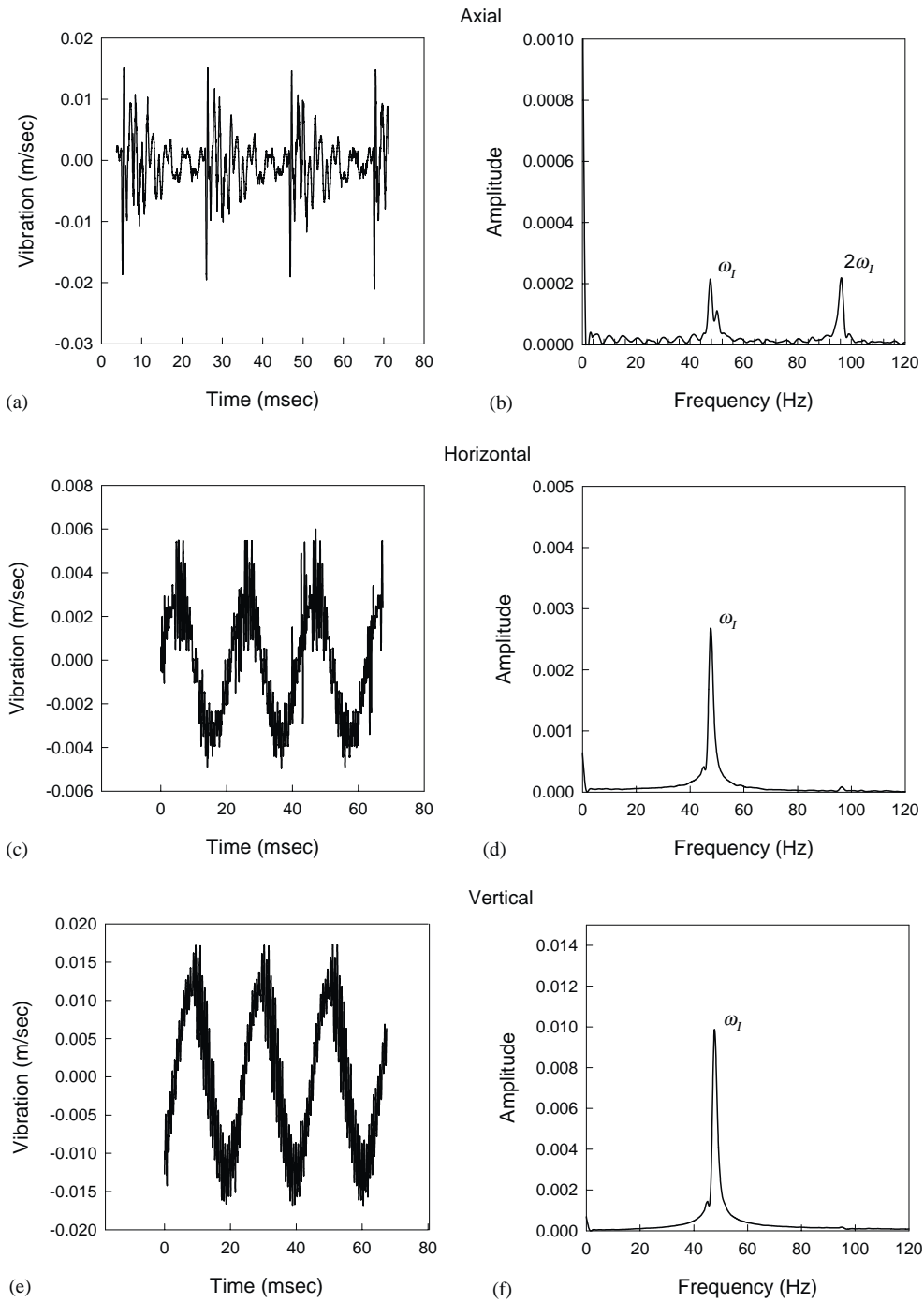
Fig. 8. Time domain and frequency domain response of cracked rotor in non-rotating condition subjected to periodic impulse excitation: (a,b) axial; (c,d) horizontal; (e,f) vertical.

domain signals in horizontal and vertical directions are quite different compared to those for the case of the uncracked shaft (Fig. 8c and e). They now show a dominant excitation frequency (46.4 Hz) together with high-frequency components (Fig. 8c and e). These high-frequency vibration components could be related to the longitudinal natural frequency and its subharmonics. Such subharmonics ($\frac{1}{2}$, $\frac{1}{4}$ and $\frac{1}{8}$ the fundamental longitudinal natural frequency) are reported to have been observed in the lateral vibration spectrum of LP rotor of a 300 MW steam turbine of the Lavrion Station of the Public Power Corporation, Greece, in 1983 [13]. The frequency spectra in both vertical and horizontal directions show presence of strong bending natural frequency component (Fig. 8d and f). In the vertical direction the amplitude of this frequency is almost 25 times that for the uncracked shaft (0.0004 in Fig. 7f as against 0.01 in Fig. 8f). In the horizontal direction this amplitude is nearly 10 times that for the uncracked shaft (0.0003 in Fig. 7d as against 0.00267 in Fig. 8d). Finally, it must be noted that the amplitude corresponding to the bending natural frequency in the case of the uncracked shaft is obviously negligible and not of any representative nature. However, the same in the case of cracked shaft is quite predominant.

The above results on both uncracked (Fig. 7) and cracked shafts (Fig. 8) establish the phenomenon of coupling of bending and axial vibrations in the case of a cracked shaft in a non-rotating condition. This is somewhat similar to the experiments in Ref. [14] wherein the longitudinal excitation frequency when matched with the flexural natural frequency during a sweep excitation, caused the resonant flexural natural frequency to appear in the lateral frequency spectrum. This feature is almost absent in the case of the uncracked shaft wherein the axial frequency component in lateral vibration spectrum showed only marginal presence compared to the cracked shaft. In case of the cracked shaft the axial excitation frequency that is made to coincide with the shaft bending natural frequency appeared quite prominently in the lateral vibration spectrum as it excited a resonance condition in lateral vibration.

Fig. 9 shows the frequency spectra for a larger frequency range of the axially excited non-rotating cracked and uncracked rotors. In fact these spectra are the same as those shown in Fig. 7b, d, f and Fig. 8b, d and f except that the frequency range is widened from 120 to 1750 Hz. The frequency spectra for the uncracked rotor in horizontal (Fig. 9c) and vertical (Fig. 9e) directions show a relatively weak axial excitation frequency component (46.4 Hz) as well as weak high frequency axial vibration frequency components (between 500 and 750 Hz). However, in case of the cracked rotor, the axial excitation frequency is very prominently seen in both lateral vibration spectra (Fig. 9d and f). Compared to the uncracked rotor there is also a relatively noticeable presence of the axial vibration frequencies (between 1250 and 1750 Hz).

4.2. Rotating shaft

The uncracked rotor rotated at a slow speed (276 r.p.m) approximately equalling 1/10th of the critical speed of lateral vibration. Fig. 10 shows time domain and frequency domain signals for the uncracked rotor rotating at a constant speed of 4.6 Hz without subjecting it to any axial excitation. The time domain signal (Fig. 10a and c) is dominant with rotational frequency of 4.6 Hz along with a high-frequency vibration although of a considerably smaller amplitude. This is clearly seen in horizontal and vertical vibration spectra of the uncracked rotor (Fig. 10b and d). These spectra show prominent presence of $1x$ component, i.e., rotational frequency ω. However,
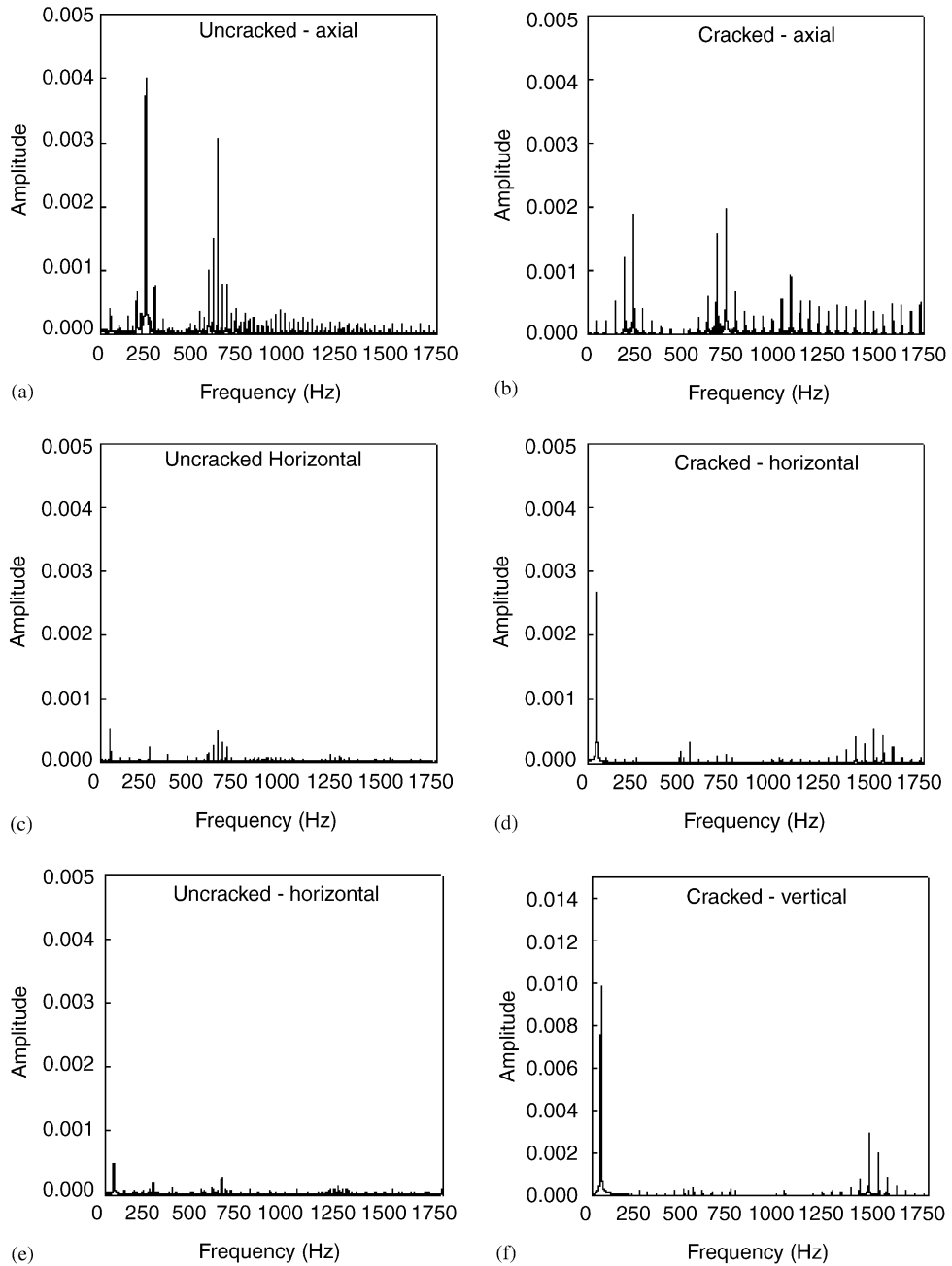
Fig. 9. Comparison of frequency domain response of the uncracked shaft and the cracked shaft in non-rotating condition subjected to periodic impulse excitation, $\omega_I = \omega_0$: (a,b) axial; (c,d) horizontal; (e,f) veritical; (a,c,e) uncracked shaft; (b,d,f) cracked shaft.
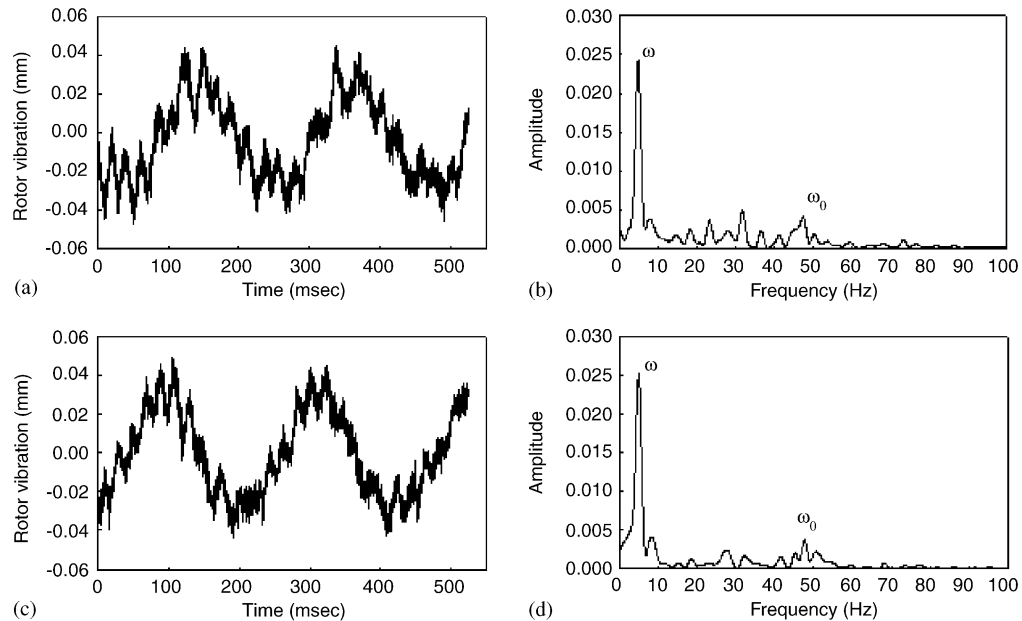
Fig. 10. Time domain and frequency domain response of the uncracked shaft without axial excitation: (a,b) horizontal; (c,d) vertical.

the higher harmonics ($2x$, $3x$, $4x$, etc.) are not quite clearly noticed. There is only a marginal representation of the $10x$ component (i.e., the bending natural frequency ω_0), and it is very weak in amplitude.

The response of the uncracked rotor to axial excitation while it is rotating at 1/10th of the critical speed of lateral vibration is shown in Fig. 11. The excitation frequency is equal to the shaft bending natural frequency. Even when the axial excitation is given, there is no significant change in the time domain (Fig. 11a and c) and frequency domain signals (Fig. 11b and d) of the system. The spectra still show dominant rotational frequency component ω and a quite small bending natural frequency component ω_0. Thus, from comparison of Figs. 10 and 11, it is clearly seen that there is neither a qualitative nor a quantitative change in the vibration response with or without axial excitation of uncracked rotor.

Next the cracked rotor is rotated at the frequency of 1/10th of the rotor bending critical speed (approximately 44 Hz). Fig. 12 shows the time domain and frequency domain signals in horizontal and vertical directions. There is no axial excitation in this case. The spectra in both horizontal (Fig. 12b) and vertical (Fig. 12d) directions show prominent presence of the $1x$ component of vibration. In addition, a very noticeable presence of higher harmonics like $2x$, $3x$ and $4x$ is seen in both the spectra. The $10x$, i.e., the bending natural frequency component of vibration is seen in the spectrum and it is comparable in magnitude with the first few harmonics of the rotational frequency ω.

The rotor bending natural frequency that matches with the $10x$ component of vibration, does make a notable appearance in the spectrum (Fig. 12b and d). This is due to the fact that the unbalance excitation at the rotational frequency of 1/10th of the critical speed together with the
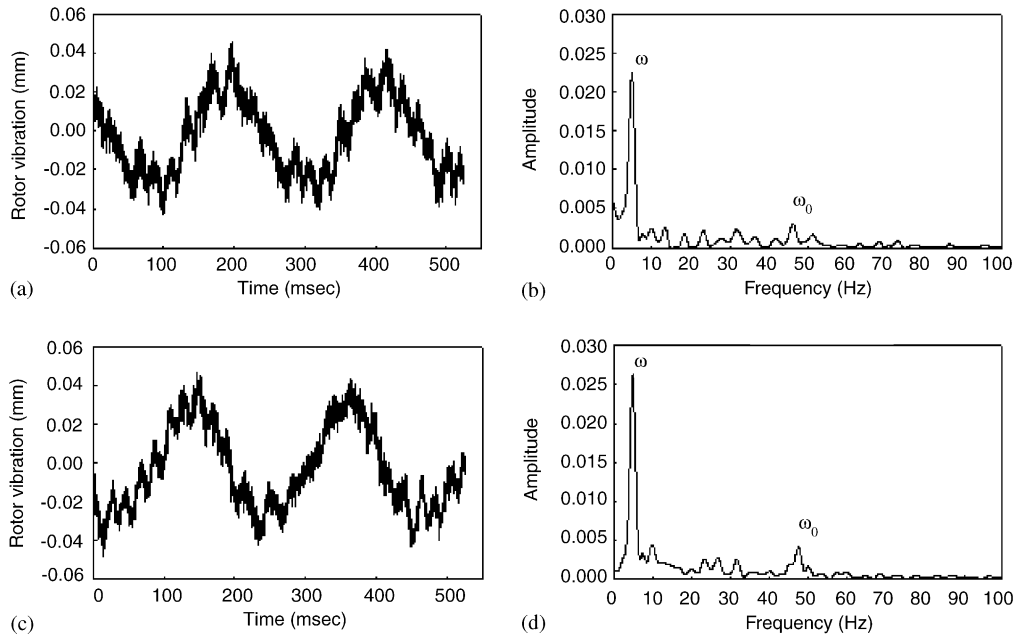
Fig. 11. Time domain and frequency domain response of the uncracked shaft with axial excitation ($\omega_I = \omega_0$): (a,b) horizontal; (c,d) vertical.
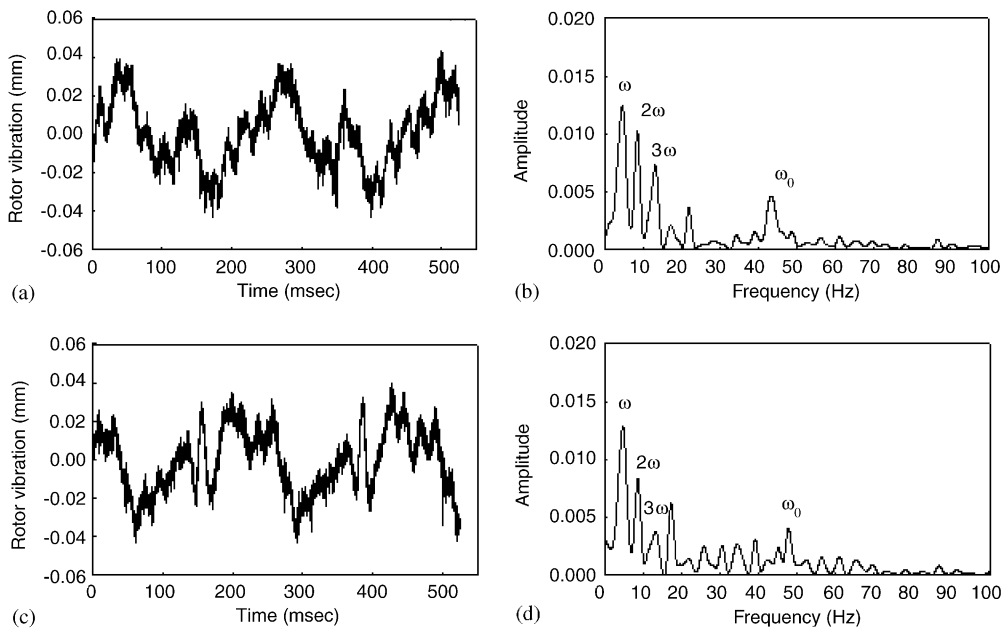

Fig. 12. Time domain and frequency domain response of the cracked rotor without axial excitation: (a,b) horizontal; (c,d) vertical.

higher harmonics due to the non-linearity of the crack can lead to the appearance of ω_0 in the spectrum. This is despite the fact that the unbalance excitation at such a low speed is weak. It may also be noted from the spectra in Fig. 12b and d that due to the non-linearity owing to the presence of crack, the cracked rotor generates $1x$, $2x$, $3x$ and higher harmonic component of vibration quite prominently. These higher harmonics were absent in the case of the uncracked rotor.

The cracked rotor rotating at 258 r.p.m (4.4 Hz) is now subjected to axial excitation at the frequency of 44 Hz (with 10 impulses per rotation) which is equal to its bending natural frequency. The resulting resonating conditions are clearly seen in the time domain signals (Fig. 13a and c). In these figures a dominant high-frequency component (the excitation frequency) is seen superposed on the low-frequency rotational speed component. The corresponding frequency domain signals (Fig. 13b and d) show a very distinct peak corresponding to the natural frequency in bending vibration of the cracked rotor. The axial excitation interacts with the bending vibration due to coupling of these vibrations in the case of the cracked rotor. The resonance is effected in lateral bending vibration because the axial excitation is given at a frequency equal to the bending natural frequency. The rotational frequency component and its harmonics in case of the excitation case (Fig. 13b and d) are almost equal in magnitude when compared with the no-excitation case (Fig. 12b and d). However, the amplitude of the bending natural frequency shows an increase by 6.8 times (from 0.00417 to 0.0283 mm) in horizontal direction and by 3 times (from 0.00403 to 0.01236 mm) in vertical direction (Figs. 12b, d, and Fig. 13b, d). It may also be noted (from Figs. 13b and d) that the bending natural frequency component ω_0 in horizontal direction is
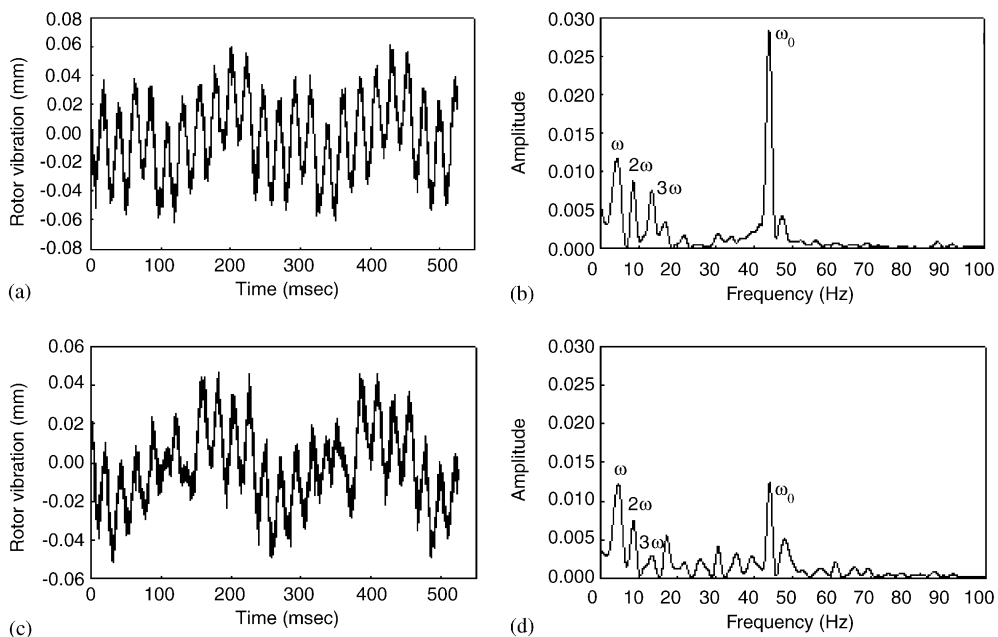

Fig. 13. Time domain and frequency domain response of the cracked rotor to axial excitation ($\omega_I = \omega_0$): (a,b) horizontal; (c,d) vertical.
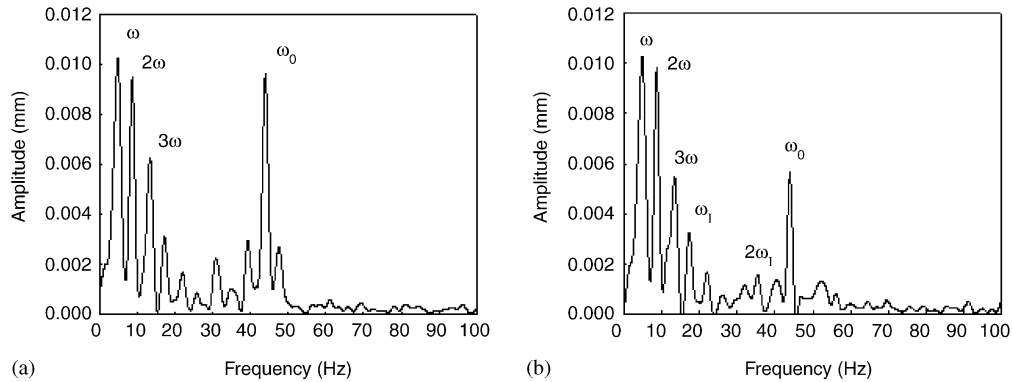
Fig. 14. Frequency spectra showing effect of axial impulse excitation on the lateral vibration response of the cracked rotor: (a) single impulse per rotation; (b) four impulses per rotation.

almost twice that in the vertical direction. In the no-excitation case (Fig. 12b and d) the frequency components in both the horizontal and vertical directions are practically identical in magnitudes.

In the next case a single impulse per rotation is applied to the cracked rotor. Fig. 14a shows the frequency spectrum obtained for the case of a single impulse per rotation in the horizontal direction. The spectrum shows the presence of the bending natural frequency in the spectrum despite the fact that the axial excitation frequency (which is now equal to ω) is not matching with the bending natural frequency (ω_0). Although the bending natural frequency component is not as strong as in the case when $\omega = \omega_0$ (Fig. 13), it is still quite prominent. The side bands around ω_0 are also clearly seen as also the first few harmonics of rotational frequency (ω, 2ω, 3ω, etc.). In this case, the single impulse per rotation causes one of the higher harmonics of excitation frequency ω to interact with the bending natural frequency due to the presence of the coupling of axial–bending vibrations. The higher harmonics appear due to non-linearity owing to a breathing crack.

Fig. 14b shows the spectrum for the case when four impulses per rotation are applied to the cracked rotor. Here the axial excitation frequency is $\omega_I = 4\omega$ and is seen in the spectrum as also the second harmonic of the excitation frequency $2\omega_I$. The existence of the bending natural frequency is noticeable but not as much prominently as in the previous cases. Due to the non-linearity owing to the presence of crack, higher harmonics are present in the vibration signal. Hence the excitation frequency ω_I and its harmonics like $2\omega_I$ are modulated by not only the rotational frequency ω, but also by its harmonics such as 2ω, 3ω, etc. This leads to the presence of sum and difference frequencies such as $\omega_I \pm \omega$, $\omega_I \pm 2\omega$, $2\omega_I \pm \omega$, $2\omega_I \pm 2\omega$. In the present case, the frequency component $2\omega_I + 2\omega$ matches with the bending natural frequency ω_0 that leads to the condition of resonance in the lateral vibration.

The experimental results presented in this section corroborate the analytical findings of a cracked Jeffcott rotor discussed in Section 2 and are summerised below.

(1) The coupling of longitudinal and bending vibrations was clearly established from theoretical analysis from the fact that bending natural frequency in the lateral vibration spectrum appeared very prominently in the case of cracked rotor (Figs. 4 and 5). This frequency (ω_0) did not show its presence in the case of uncracked rotor. This observation is confirmed in the

present experimental work from the very prominent ω_0 frequency component in the case of cracked rotor (Figs. 13 and 14) and comparatively negligible magnitude of this frequency in the uncracked rotor (Fig. 11).

(2) It has been shown theoretically in Section 2 that when the axial excitation frequency (ω_I) matched with the bending natural frequency (ω_0), the resonating conditions were effected leading to the dominant presence of bending natural frequency in the lateral vibration spectrum (Fig. 5). Due to modulations caused by the rotational frequency, the side bands appeared around the bending natural frequency. In the experimental results, this is clearly observed in Fig. 13.

(3) The bending natural frequency component in horizontal direction is larger than that in the vertical direction (Fig. 5). From the experimental results (Fig. 13), it is seen that the horizontal component is almost two times the component in vertical direction.

(4) When axial excitation is given in the form of single impulse per rotation ($\omega_I = \omega$), the bending natural frequency appears in the lateral vibration spectrum (Fig. 4a) although its amplitude is small as compared to the case when $\omega_I = \omega_0$. This analytical finding is also confirmed from Fig. 14a in which bending natural frequency component (ω_0) is less than half (0.0097 as against 0.0283) compared to the case when $\omega_I = \omega_0$ (Fig. 13b).

(5) When more number of impulses are applied per rotation (say 4 impulses per rotation) so that the axial excitation frequency $\omega_I = 4\omega$, the axial excitation frequency and its harmonics appear in the lateral vibration spectrum (Fig. 4b). In addition to these, side bands due to interaction of rotational frequency ω and its harmonics (2ω, 3ω, etc.) with the axial excitation frequency ω_I and its harmonics ($2\omega_I$, $3\omega_I$, etc.) also appear in the lateral vibration spectrum. This feature is also observed in the experimental finding of this section (Fig. 14b) in which both ω_I and $2\omega_I$ are seen and the side frequency $2\omega_I + 2\omega$ excited the bending natural frequency in the lateral vibration.

The authors are of the view that the influence of the axial excitation on the lateral vibrations would also be observed for lower crack depths of say $\bar{a} = 0.1$. This is particularly because such influence is quite prominently observed for $\bar{a} = 0.23$ in the experimental results here and also from the fact that the theoretical study in Ref. [17] has shown that the bending natural frequency component for $\bar{a} = 0.1$ is approximately half of that for $\bar{a} = 0.2$. It may also be noted that in this experimental investigations the bending natural frequency component for the cracked shaft ($\bar{a} = 0.23$) has increased 25 times in stationary condition and by almost 7 times in rotating condition compared to its amplitude for the uncracked rotor.

5. Conclusions

Detailed experimental investigations on the response of the cracked rotor to axial impulse excitation are carried out. The response in both non-rotating and rotating conditions are studied. The following conclusions are drawn:

1. The presence of axial excitation frequencies in the spectrum of lateral vibrations for a cracked shaft is established experimentally. Experimental investigations in the case of both rotating and

non-rotating conditions confirm this fact. There is only marginal presence of the axial frequencies in the lateral vibration spectra of an uncracked shaft. In the case of cracked shaft the prominent presence of these axial frequencies in the lateral vibration spectra confirms the coupling of bending and longitudinal vibrations.

2. In non-rotating condition, the cracked shaft showed the presence of the axial excitation frequency in the spectrum of lateral vibration thereby confirming the presence of coupling of axial and bending vibrations in the case of cracked shaft. When such excitation under similar conditions is given to the uncracked shaft the presence of the axial frequencies in the lateral vibrations was marginal. The amplitude of the axial excitation frequency component in the lateral vibration spectra of the cracked shaft was 10–25 times that in the case of uncracked shaft.

3. When the rotors are axially excited in the rotating condition with the frequency equal to the bending natural frequency, the bending natural frequency showed prominent presence in both horizontal and vertical lateral vibration spectra. The bending natural frequency is found to be twice as strong in the horizontal direction than in the vertical direction.

4. From the various cases studied (single, four, ten impulses per rotation), it is shown that the bending natural frequency (ω_0) could be excited by

 (i) matching any one of the harmonics of the axial excitation frequency ($\omega_0 = n\omega_I$).

(ii) matching any of the sum and difference combination frequencies ($\omega_0 = n\omega_I \pm m\omega$).

5. The non-linearity due to the crack is clearly observed with the presence of higher harmonics of the rotational frequency in the spectrum. This was found almost absent in the case of the uncracked rotor. The bending natural frequency also fails to show up in the spectrum of the uncracked rotor. This clearly confirms the coupling of bending and axial vibrations in the case of cracked rotor that is absent in the case of uncracked rotor.

The above findings are expected to supplement the crack detection process in a rotor by utilising the response of rotor to axial excitation, particularly during slow roll conditions.

Appendix A. Nomenclature

a	depth of crack
D	diameter of the shaft
$\bar{a}$	crack depth ratio (a/D)
L	length of the shaft
m	mass of the disc
ε	eccentricity of mass of disc from its geometric centre
δ_{st}	static deflection of the rotor
e	dimensionless eccentricity (ε/δ_{st})
β	orientation of eccentricity from ξ-axis in the direction of shaft rotation
ζ	damping factor
E	modulus of elasticity
$\theta(t)$	instantaneous angle of rotation of shaft

y, z	dimensional rotor displacement in vertical and horizontal direction, respectively
$\bar{y}, \bar{z}$	non-dimensional rotor displacement in vertical and horizontal direction, respectively
ξ, η	dimensional rotor centre displacement in the direction perpendicular to crack edge and in the direction parallel to crack edge, respectively
$\bar{\xi}, \bar{\eta}$	non-dimensional rotor centre displacement in the direction perpendicular to crack edge and in the direction parallel to crack edge, respectively
$u, \bar{u}$	dimensional and non-dimensional rotor displacement in longitudinal direction
τ	dimensionless time
ω	rotational frequency
ω_0	natural frequency of lateral vibration of the rotor
ω_I	impulse excitation frequency
r_{unb}	dimensionless speed of rotation (ω/ω_0)
k_0	stiffness of the shaft without crack
k_ξ, k_η, k_u	direct stiffness of the shaft in ξ, η and u direction, respectively
$k_{\xi u}, k_{\xi\eta}, k_{\eta u}, k_{\eta\xi}, k_{u\xi}, k_{u\eta}$	cross-coupled stiffnesses
Q_ξ, Q_η, Q_u	forces acting on the shaft in ξ, η and u direction, respectively

References

[1] J. Schmied, E. Kramer, Vibrational behaviour of a rotor with a cross-sectional crack. in: International Conference on Vibrations in Rotating Machinery 3, Institution of Mechanical Engineers Publications, London, 1984, pp. 183–192.

[2] W. Mayes, W.G.R. Davies, Analysis of the response of the multi-rotor-bearing system containing a transverse crack in a rotor, Journal of Vibration, Acoustics, Stress, and Reliability in Design 106 (1984) 139–145.

[3] N. Bachschmid, G. Diana, B. Pizzigoni, The influence of unbalance on cracked rotors, in: International Conference on Vibrations in Rotating Machinery 3, Institution of Mechanical Engineers Publications, 1984, London.

[4] B. Grabowski, The vibrational behaviour of a rotating shaft containing a transverse crack, in: O. Mahrenhotz (Ed.), Dynamics of rotors - Stability and system identification. CISM Courses & Lectures, Vol. 273, Springer, New York, 1984, pp. 423–465.

[5] I. Imam, S.H. Azzaro, R.J. Bankert, J. Scheibel, Development of an on-line rotor crack detection and monitoring system, Journal of Vibration, Acoustics, Stress and Reliability in Design 111 (1989) 241–250.

[6] O.S. Jun, H.J. Eun, Y.Y. Earmme, C.W. Lee, Modelling and vibration analysis of a simple rotor with a breathing crack, Journal of Sound and Vibration 155 (1992) 273–290.

[7] M.C. Wu, S.C. Huang, In-plane vibration and crack detection of a rotating shaft-disk containing a transverse crack, Journal of Vibration and Acoustics 120 (1998) 551–556.

[8] C.A. Papadopoulos, A.D. Dimarogonas, Coupling of bending and torsional vibration of a cracked Timoshenko shaft, Ingenieur-Archiv 57 (1987) 257–266.

[9] A. Muszynska, P. Goldman, D.E. Bently, Torsional/lateral vibration cross-coupled responses due to shaft anisotropy: a new tool in shaft crack detection, in: International Conference on Vibrations in Rotating Machinery 5, Institution of Mechanical Engineers Conference Publications, London, 1992, pp. 257–262.

[10] W.M. Ostachowicz, M. Krawczuk, Coupled torsional and bending vibrations of a rotor with an open crack, Archive of Applied Mechanics 62 (1992) 191–201.

[11] C.A. Papadopoulos, A.D. Dimarogonas, Coupled longitudinal and bending vibrations of a rotating shaft with an open crack, Journal of Sound and Vibration 117 (1987) 81–93.

[12] A. Papadopoulos, A.D. Dimarogonas, Coupled vibration of cracked shafts, Journal of Vibration and Acoustics 114 (1992) 461–467.

[13] C.A. Papadopoulos, A.D. Dimarogonas, Stability of cracked rotors in the coupled vibration mode, Journal of Vibration, Acoustics, Stress and Reliability in Design 110 (1988) 356–359.

[14] C.A. Papadopoulos, A.D. Dimarogonas, Coupled longitudinal and bending vibration of a cracked shaft, Journal of Vibration, Acoustics, Stress and Reliability in Design 110 (1988) 1–8.

[15] T. Iwatsubo, S. Arii, A. Oks, Detection of a transverse crack in a rotor shaft by adding external force, in: International Conference on Vibrations in Rotating Machinery 5, Institution of Mechanical Engineers Conference Publications, London, 1992, pp. 275–282.

[16] K.R. Collins, R.H. Plaut, J. Wauer, Detection of cracks in rotating Timoshenko shafts using axial impulses, Journal of Vibration and Acoustics 113 (1991) 74–78.

[17] A.K. Darpe, A. Chawla, K. Gupta, Analysis of the response of a cracked Jeffcott rotor to axial excitation, Journal of Sound and Vibration 249 (2002) 429–445.

[18] A. Tondl, Some Problems of Rotor Dynamics, Publishing House of the Czechoslovac Academy of Sciences, Prague, 1965.